JACS
JOURNAL OF THE AMERICAN CHEMICAL SOCIETY

Communication

pubs.acs.org/JACS

Interfacial Fabrication of Single-Crystalline ZnTe Nanorods with High Blue Fluorescence

Linrui Hou, Qiang Zhang, Luting Ling, Chen-Xiong Li, Li Chen, and Su Chen*

State Key Laboratory of Materials-Oriented Chemical Engineering, and College of Chemistry and Chemical Engineering, Nanjing University of Technology, Nanjing 210009, P. R. China

Supporting Information

ABSTRACT: From the perspective of practical application, the development of fluorescent nanocrystals with low toxicity and desirable optical properties is highly needed. Here we report a new liquid–liquid interfacial synthesis of single-crystalline ZnTe nanorods with high fluorescence. With the use of long-alkyl-chain fatty acid as the capping ligand, the reaction of zinc acrylate with NaHTe under a moderate temperature (~90 °C) at the toluene/water interface yielded high-quality ZnTe nanorods. The preparation parameters and the growth mechanism were thoroughly investigated. The as-prepared ZnTe nanorods exhibited stable blue fluorescence with quantum yield up to 60%. This bright and stable emission gives promise for the use of these relatively benign nanorods in various applications such as blue light-emitting diodes.

Semiconductor nanocrystals (NCs) have received considerable attention over the past two decades, owing to their unique optical and electronic properties and their promising applications in optoelectronic devices, biological labeling, and imaging.[1−3] Zinc telluride (ZnTe), with a direct bandgap of 2.26 eV (~548 nm) at room temperature, is an attractive semiconductor for optoelectronic applications, such as green light-emitting diodes (LEDs) or solar cells.[4,5] Particularly, compared with other semiconductor including cadmium chalcogenides and lead chalcogenides, ZnTe is more desirable for health and environment concerns without potential leakage of heavy-metal ions. Nevertheless, rather few works of the preparation of nanocrystalline ZnTe can be indexed,[4,6−9] probably due to the lack of appropriate precursors and synthetic approaches. Meanwhile, it is still a challenge to prepare anisotropic shapes of semiconductor NCs.[10−12] Although several 1D ZnTe NCs have been achieved in organic solution by tuning the reaction conditions, they have diameters much larger than the Bohr exciton radius of 6.2 nm and thus fail to exhibit quantum confinement effects.[5,13−17] Most recently, Zhang et al. successfully fabricated the wurtzite ZnTe nanorods with smaller dimension (<7 nm), while no photoluminescence (PL) was observed due to the longer-lived charge separated state.[8]

We demonstrate the first interfacial synthesis of fluorescent ZnTe nanorods possessing the following notable characteristics: (1) facile generation at the liquid–liquid interface under a moderate temperature of ~90 °C; (2) high-quality single-crystalline nanorod structure; (3) bright blue fluorescence with good stability and highest quantum yield (QY, ~60%) reported to date for ZnTe NCs; and (4) versatile application in such as blue LED devices. The single-crystalline ZnTe nanorods with remarkable quantum confinement effects are still scarcely reported, and this work contributes an available low-temperature synthetic strategy to prepare high-quality anisotropic shapes of semiconductor NCs with desirable optical properties potentially useful in optoelectronic, sensory, and biomedical areas.

Synthesis of ZnTe nanorods proceeds via reaction of zinc acrylate [$Zn(AA)_2$] with NaHTe in the presence of oleic acid (OA) as capping ligand under 90 °C at the toluene/water interface. A liquid–liquid interface is an ideal platform for efficient fabrication of NCs with diverse structures driven by a minimization of interfacial energy.[2,18−20] Typically, OA (6 mmol) dissolved in toluene (20 mL) was added dropwise into 30 mL of toluene containing $Zn(AA)_2$ (1 mmol) under vigorously stirring for 1 h, followed by the addition of water (50 mL) to form liquid–liquid biphase system, which was degassed with N_2 for 30 min. Then 1 mL of aqueous solution of fresh NaHTe (0.5 mmol) was injected dropwise into the above N_2-saturated biphase solution. After stirring for additional 2 h, the mixture was heated at 90 °C for 4 h to obtain OA-capped ZnTe nanorods, referred to as ZnTe-OA nanorods.

The interfacial synthetic strategy allows the fabrication of highly fluorescent single-crystalline ZnTe nanorods. Figure 1a,b show the transmission electron microscopic (TEM) images of as-prepared ZnTe-OA nanorods. Obviously, the resultant product has rod-like nanostructure with the lengths of 10−20 nm and average diameter of ~3 nm. The selected area electron diffraction (SAED) pattern indicates its typical single-crystalline nature and can be indexed as the cubic structure of ZnTe (Figure 1c). Careful examination of the corresponding high-resolution transmission electron microscopic (HRTEM) image of the ZnTe-OA nanorod reveals the well-resolved lattice fringes with an inter plane distance of 0.31 nm (Figure 1d), which matches well with the expected *d*-spacing of the (220) crystal plane of cubic ZnTe crystal. Thus, the as-fabricated single-crystalline ZnTe nanorods grow along the [200] crystal direction. The X-ray diffraction (XRD) analysis further confirms the cubic structure of ZnTe (JCPDS card no. 15-0746, space group $F\bar{4}3m$ [216], a = 6.103 Å).[6] Significantly, the as-prepared ZnTe-OA nanorods show good optical properties (Figure 1f). Compared with bulk ZnTe with the band gap of

Received: May 12, 2013
Published: July 8, 2013

dx.doi.org/10.1021/ja4047476 | J. Am. Chem. Soc. 2013, 135, 10618−10621

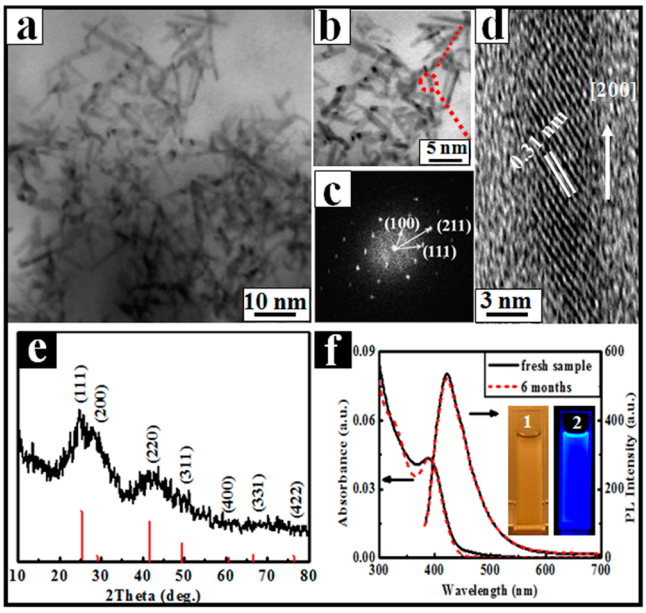

Figure 1. (a) TEM and (b) HRTEM images and (c) SAED pattern of ZnTe-OA nanorods. (d) HRTEM image of a single ZnTe-OA nanorod indicated by the red circle in (b). (e) XRD pattern of ZnTe-OA nanorods. (f) Absorption and emission spectra (λ_{ex} = 380 nm) of toluene solution of ZnTe-OA nanorods: fresh (solid lines) and stored for one-half year (dashed lines). Inset: digital photographs of toluene solution of ZnTe-OA nanorods taken under daylight (1) and 365 nm UV light (2).

2.26 eV (548 nm), the ZnTe nanorods exhibit obvious blue shift of the emission peak (423 nm), which should be ascribed to quantum confinement effects. The QY was calculated to be about 60%, which is the highest reported to date for fluorescent ZnTe NCs. In addition, the sample showed no obvious change in PL spectra after being stored under ambient conditions for 6 months (Figure 1f), revealing the good stability of fluorescence. The excellent PL properties in terms of brightness and stability are meaningful for further applications of ZnTe-OA nanorods.

To gain insight into the synthesis of NCs at the biphase interface, the effect of the reaction variables on the formation and the PL properties of ZnTe nanorods were systematically investigated, including the excitation wavelength, the role of OA, the species of zinc precursors, the injecting timing of NaHTe, and the temperature and duration of heat treatment. To investigate the role of OA in the formation of ZnTe nanorods, a control experiment was conducted in the absence of the stabilizing ligand. Upon injecting NaHTe into the $Zn(AA)_2$ solution, a large amount of black precipitates formed immediately. Similar phenomena were also observed for the thiolglycolic acid-capped CdTe NCs, owing to the detachment of thiol ligands from the surface of NCs.[21,22] Nevertheless, the deficiency of ligands may be the inherent reason for the formation of black precipitates in our case. The black sample was determined to be the insoluble Te powder possessing spherical nanostructure with diameter of ~4 nm (Figures S2 and S3) rather than ZnTe NCs, owing to the rapid oxidization of ZnTe NCs into Te species after exposed to the air. Therefore, the stabilizing ligand unambiguously plays a great role in the formation of ZnTe nanorods. Furthermore, only moderate amount of OA ($Zn(AA)_2$:OA = 1:6 mol/mol) can provide effective passivation for NC surface to give desirable PL properties (Figure S4).

Six reagents including $Zn(Ac)_2{\cdot}2H_2O$, $Zn(NO_3)_2{\cdot}6H_2O$, $ZnSO_4{\cdot}7H_2O$, $ZnCl_2$, $Zn(AA)_2$, and $Zn[CH_3(CH_2)_{16}COO]_2$ [$Zn(SA)_2$] were chosen in our case to fabricate ZnTe NCs. However, only successful synthesis of ZnTe NCs was realized by using $Zn(AA)_2$ as the zinc source. The reason might be associated with the different solvency of these zinc sources in water: $ZnSO_4{\cdot}7H_2O$ ($Zn(NO_3)_2{\cdot}6H_2O$ and $ZnCl_2$) > $Zn(Ac)_2{\cdot}2H_2O$ > $Zn(AA)_2$ > $Zn(SA)_2$. With the use of water-soluble inorganic salts $Zn(NO_3)_2{\cdot}6H_2O$, $ZnSO_4{\cdot}7H_2O$, $ZnCl_2$, and $Zn(Ac)_2{\cdot}2H_2O$ as zinc source, Zn^{2+} reacts with HTe^- in aqueous phase, resulting the similar phenomena as that in the case of absence of OA described above. ZnTe NCs with different shapes were synthesized by using $Zn(SA)_2$ in organic solution, while the dimension of the ZnTe nanorods is too large to exhibit quantum confinement effects.[16] $Zn(SA)_2$ is also not a desired zinc source in water/toluene biphase system because it never comes close to water phase. The key reason that $Zn(AA)_2$ can be used successfully in the interfacial synthesis probably is its slight solubility in water enabling its slow reaction with NaHTe in the water region of the interface. Then small ZnTe clusters produced from slow nucleation are being surrounded by OA and transported into the toluene phase by interaction with OA. The organic ligand OA bound to the NC surface can provide effective passivation for NCs, thus the obtained NCs can be endowed with resistance toward oxidation.

The injecting timing and the heat treatment conditions were also investigated. By applying the conventional injecting timing period for NaHTe,[23] the obtained ZnTe NCs display extremely weak stability. The oxidation of ZnTe into the Te phase was observed upon injecting NaHTe solution at 90 °C. Alternatively, we injected the NaHTe solution at room temperature. Although the obtained product shows weak PL properties, the heat treatment of NCs at certain temperature can improve their crystal degree and thus their PL properties.[23] The NCs heated to 70−100 °C for proper time show the obviously improved PL properties in comparison with those at room temperature (Figure S5). We noted that the decrease in PL was observed when the heating temperature was increased to 100 °C. Higher temperature might result in the detachment of the excessive ligands from the NC surface and an increase in the formation rate of complexes, which would cause an obvious decrease in PL intensity.[24] The PL intensity maximum appears under heating duration of 4 h (Figure S6). Thus, the optimum heating temperature and duration herein are 90 °C and 4 h, which is significantly lower than those adopted in conventional organic synthesis.[23−25]

TEM analysis on the products obtained at different time intervals was further carried out to explore the formation mechanism of the nanorods. At room temperature, the NCs with the diameters of 1−2 nm are dominant in the obtained sample (Figure 2a). Generally, for the NCs with cubic crystal structure, it is difficult for them to form anisotropic nanostructures in view of the classical Ostwald ripening mechanism.[11] Interestingly, only after heat treatment for 10 min, aggregated nanoparticles are formed along with some nanorods with the diameters and lengths of 1−2 nm and 3−5 nm, respectively (Figure 2b). When the heating duration exceeds 1 h, nanorods with diameter of ~3 nm and length >10 nm were obtained (Figure 2c). As the heating duration increases to 12 h, the dimension of the nanorods elongates to ~12 × 150 nm (Figure 2d). ZnTe nanorods obtained after refluxing for 12 h clearly show the single-crystalline feature

dx.doi.org/10.1021/ja4047476 | J. Am. Chem. Soc. 2013, 135, 10618−10621

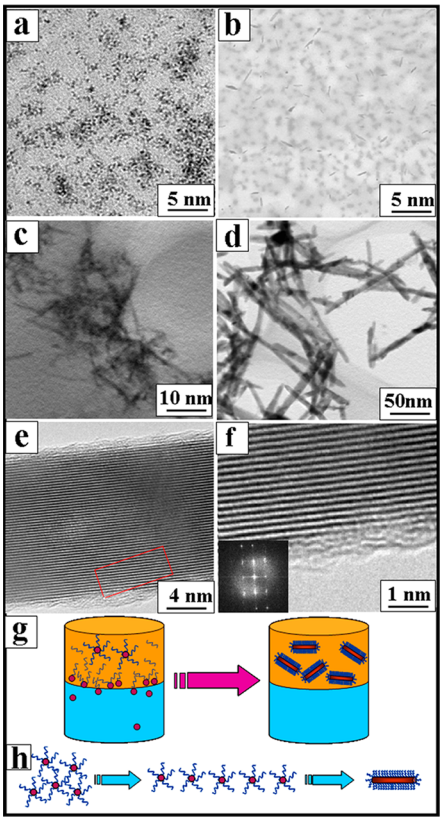

Figure 2. TEM images of ZnTe-OA NCs obtained from different synthetic stages: before heating (a) and after heating at 90 °C for 10 min (b), 1 h (c), and 12 h (d). (e) HRTEM image of a single ZnTe-OA nanorod selected from the sample (d). (f) HRTEM image of the region indicated by the rectangle in (e). Inset in (f) showing the corresponding SAED pattern. (g) Schematic illustration of the preparation route forming the ZnTe Nanorods. (h) Proposed formation mechanism of the oriented aggregation of NCs into nanorods.

(Figure 2e,f). Meanwhile, the adherence of OA on the surfaces of nanorods can also be seen from Figure 2e,f. This peculiarity undoubtedly confers ZnTe nanorods with improved stability. Further investigation reveals that the pearl-necklace-like nanostructures were obtained in the early stage of the formation of ZnTe nanorods (Figure S7), wherein the nanorod constituting several attached NCs can be clearly observed. Recently, some cubic NCs, such as CdTe,[26] PbSe,[27] and CdS,[18,28] have been assembled into anisotropic nanostructures based on the oriented attachment mechanism, in which the dipolar−dipolar interaction is the most probable driving force to induce the NCs to assemble into the chain-like microstructures. Besides, the anisotropic attractive interaction also includes van der Waals interactions.[29,30] According to the oriented attachment mechanism, the diameter of the nanorods should keep uniformity with that of the attached nanoparticles. However, in our case, on prolonging the duration of heat treatment, both of the length and diameter of nanorods increase. Obviously, Ostwald ripening simultaneously plays an important role during the shape evolution process of NCs.

According to the above observations, a schematic illustration to visualize the growth mechanism is displayed in Figure 2g,h. Upon injecting aqueous solution of NaHTe into the biphase system, $Zn(AA)_2$ reacts with NaHTe at the biphase interface. Then the ligand molecule OA is adsorbed to the generated NC surfaces, which drags the NCs into toluene phase due to hydrophobicity of alkyl chain in OA. When NCs approach each other closely under dipolar force and van der Waals interactions, they can rearrange to realize the low-energy configuration due to the tendency of minimizing their surface areas associated with the high-energy facets. Then the NCs aggregate into pearl-necklace-like chain due to oriented attachment mechanism, through which the NCs almost end-to-end fused along certain direction to form linear chains and change from polycrystalline to single-crystalline structure. Simultaneously, Ostwald ripening also plays a great role in causing the growth of nanorods in both diameter and length.

It is worth noting that the preparation of fluorescent ZnTe nanorods from the use of a long-alkyl-chain fatty acid as the capping ligand at the liquid−liquid interface we proposed might be versatile. The replacement of OA with undecylenic acid (UA) and stearic acid (SA) also results in the successful formation of ZnTe nanorods, referred to as ZnTe-UA and ZnTe-SA nanorods, respectively (Figure 3). ZnTe-UA nano-

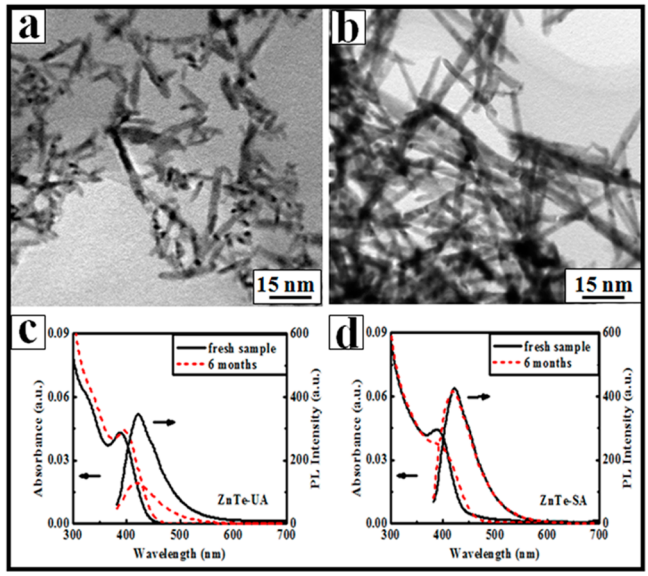

Figure 3. TEM images of (a) ZnTe-UA and (b) ZnTe-SA nanorods. (c,d) Absorption and emission spectra (λ_{ex} = 380 nm) for toluene solutions of (c) ZnTe-UA and (d) ZnTe-SA nanorods: fresh (solid lines) and after storage for one-half year (dashed lines).

rods have the diameters of 3−5 nm and lengths of 10−20 nm (Figure 3a), while the longer nanorods with the length up to ∼70 nm are produced when longer alkyl-chain ligand SA is used (Figure 3b). The UV−vis absorption and emission bands significantly blue shift in comparison with those of bulk ZnTe, demonstrating the occurrence of striking quantum confinement effects, similar to those for ZnTe-OA nanorods (Figure 3c,d). The absorption peaks are focused on ∼390 nm for both ZnTe-UA and ZnTe-SA nanorods. Both nanorods show high blue fluorescence with emission wavelengths at ∼422 nm. Additionally, ZnTe-SA nanorods showed no obvious change in PL spectra after being stored under ambient conditions for 6 months. Whereas, owing to increasing acidity trend of SA < OA < UA, the adhesion strength of the three ligands to the NCs follows the opposite trend, and hence the weaker stability for ZnTe-UA nanorods in air was observed.

Finally, to make the best of these ZnTe nanorods with the virtues of high QYs, good stability, and low toxicity, we

dx.doi.org/10.1021/ja4047476 | J. Am. Chem. Soc. 2013, 135, 10618−10621

employed the ZnTe-OA nanorods as color conversion material for the construction of LED devices. Figure 4a shows the

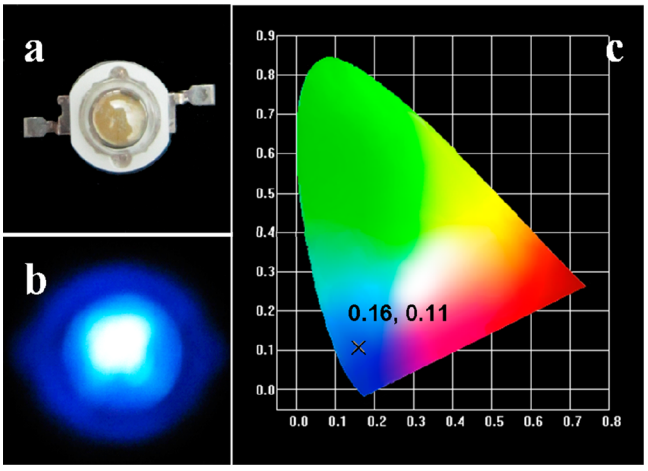

Figure 4. (a) Photographs of the LED with ZnTe-OA nanorods. (b) Emitted blue light of the LED device. (c) Placement of the ZnTe-OA emission spectra on the CIE 1931 chromaticity chart.

structure of the nanorod-based LED lamp, in which the as-prepared ZnTe-OA nanorods were employed as color converter and a UV chip as excitation source. Thermal-curing transparent silicone was also used to pack the blue emission NCs onto the chip. As shown in Figure 4b, operated at the current of 350 mA, the device provides bright blue illumination. The emission color of ZnTe nanorods can be better quantified with the Commission International d'Éclairage (CIE) 1931 chromaticity coordinates, which serves to specify how the human eye perceives light with a given spectrum. As seen in Figure 4c, the coordinates of the LEDs are located at (0.16, 0.11) belonging to the blue gamut. To the best of our knowledge, the application of ZnTe NCs in blue LED devices has not been reported before.

In summary, we report a new versatile interfacial synthetic strategy for preparing single-crystalline ZnTe nanorods with extremely narrow diameter of <6 nm under a moderate temperature. The synergistic effect of the oriented attachment and Ostwald ripening mechanism plays a great role in the formation process of nanorods. The obtained ZnTe nanorods exhibit bright blue fluorescence with good stability and high QYs (~60%), making them promising building blocks for the further development of nanodevices, such as LEDs or nanosensors. This facile approach might be easily applied to fabricate various high-quality semiconductor NCs with anisotropic shapes and good properties.

■ ASSOCIATED CONTENT

Supporting Information

Experimental details additional characterization data. This material is available free of charge via the Internet at http://pubs.acs.org.

■ AUTHOR INFORMATION

Corresponding Author

chensu@njut.edu.cn

Notes

The authors declare no competing financial interest.

■ ACKNOWLEDGMENTS

This work was supported by National Natural Science Foundation of China (21076103 and 21176122), the National High Technology Research and Development Program of China (863 Program) (2012AA030313), Specialized Research Fund for the Doctoral Program of Higher Education of China (20103221110001), and Priority Academic Program Development of Jiangsu Higher Education Institutions (PAPD).

■ REFERENCES

(1) Yin, Y. D.; Alivisatos, A. P. *Nature* **2005**, *437*, 664−670.
(2) Yang, S. Y.; Wang, C. F.; Chen, S. *J. Am. Chem. Soc.* **2011**, *133*, 8412−8415.
(3) Michalet, X.; Pinaud, F. F.; Weiss, S. *Science* **2005**, *307*, 538−544.
(4) Zhou, W. C.; Tang, D. S.; Pan, A. L.; Zhang, Q. L.; Wan, Q.; Zou, B. S. *J. Phys. Chem. C* **2011**, *115*, 1415−1421.
(5) Bhunia, S.; Bose, D. N. *J. Cryst. Growth* **1998**, *186*, 535−542.
(6) Li, Y. D.; Ding, Y.; Wang, Z. Y. *Adv. Mater.* **1999**, *11*, 847−850.
(7) Zhang, J.; Chen, P. C.; Shen, G. Z.; He, J. B.; Kumbhar, A.; Zhou, C. W.; Fang, J. Y. *Angew. Chem., Int. Ed.* **2008**, *47*, 9469−9471.
(8) Zhang, J.; Jin, S. Y.; Fry, H. C.; Peng, S.; Shevchenko, E.; Wiederredcht, G. P.; Rajh, T. *J. Am. Chem. Soc.* **2011**, *133*, 15324−15327.
(9) Xu, S. H.; Wang, C. L.; Xu, Q. Y.; Zhang, H. S.; Li, R. Q.; Shao, H. B.; Lei, W.; Cui, Y. P. *Chem. Mater.* **2010**, *22*, 5838−5844.
(10) Pradhan, N.; Xu, H. F.; Peng, X. G. *Nano Lett.* **2006**, *6*, 720−724.
(11) Peng, X. G.; Manna, L.; Yang, W. D.; Wickham, J.; Scher, E.; Kadavanich, A.; Alivisatos, A. P. *Nature* **2000**, *404*, 59−61.
(12) Lilly, G. D.; Lee, J.; Sun, K.; Tang, Z. Y.; Kim, K. S.; Kotov, N. A. *J. Phys. Chem. C* **2008**, *112*, 370−377.
(13) Jun, Y.; Choi, C. S.; Cheon, J. *Chem. Commun.* **2001**, 101−102.
(14) Yong, K. T.; Sahoo, Y.; Zeng, H.; Swihart, M. T.; Minter, J. R.; Prasad, P. N. *Chem. Mater.* **2007**, *19*, 4108−4110.
(15) Zhang, J.; Sun, K.; Kumbhar, A.; Fang, J. Y. *J. Phys. Chem. C* **2008**, *112*, 5454−5458.
(16) Lee, S. H.; Kim, Y. J.; Park, J. *Chem. Mater.* **2007**, *19*, 4670−4675.
(17) Li, L.; Yang, Y. W.; Huang, X. H.; Li, G. H.; Zhang, L. D. *J. Phy. Chem. B* **2005**, *109*, 12394−12398.
(18) Hou, L. R.; Wang, C. F.; Chen, L.; Chen, S. *J. Mater. Chem.* **2010**, *20*, 3863−3868.
(19) Yu, Z. Y.; Wang, C. F.; Ling, L. T.; Chen, L.; Chen, S. *Angew. Chem., Int. Ed.* **2012**, *51*, 2375−2378.
(20) Yu, Z. Y.; Wang, C. F.; Chen, S. *J. Mater. Chem.* **2011**, *21*, 8496−8501.
(21) Mandal, A.; Tamai, N. *J. Phys. Chem. C* **2008**, *112*, 8244−8250.
(22) Zhang, H.; Zhou, Z.; Yang, B. *J. Phys. Chem. B* **2003**, *107*, 8−13.
(23) Li, J. J.; Wang, Y. A.; Guo, W. Z.; Keay, J. C.; Mishima, T. D.; Johnson, M. B.; Peng, X. G. *J. Am. Chem. Soc.* **2003**, *125*, 12567−12575.
(24) He, Y.; Sai, L. M.; Lu, T. T.; Hu, M.; Lai, W. Y.; Fan, Q. L.; Wang, L. H.; Huang, W. *Chem. Mater.* **2007**, *19*, 359−365.
(25) Murray, C. B.; Norris, D. J.; Bawendi, M. G. *J. Am. Chem. Soc.* **1993**, *115*, 8706−8715.
(26) Tang, Z. Y.; Kotov, N. A.; Giersig, M. *Science* **2002**, *297*, 237−248.
(27) Cho, K. S.; Talapin, D. V.; Gaschler, W.; Murray, C. B. *J. Am. Chem. Soc.* **2005**, *127*, 7140−7145.
(28) Hou, L. R.; Chen, L.; Chen, S. *Langmuir* **2009**, *25*, 2869−2874.
(29) Pileni, M. −P. *Acc. Chem. Res.* **2007**, *40*, 685−693.
(30) Liu, Y. Z.; Lin, X. M.; Sun, Y. G.; Rajh, J. *J. Am. Chem. Soc.* **2013**, *135*, 3764−3767.